PERFORMANCE ANALYSIS OF ALGORITHMIC NOISE-TOLERANCE TECHNIQUES

Byonghyo Shim and Naresh R. Shanbhag

Coordinated Science Laboratory, ECE Dept.
University of Illinois at Urbana-Champaign
1308 West Main Street, Urbana, IL 61801
Email: [bshim,shanbhag]@mail.icims.csl.uiuc.edu

ABSTRACT

In this paper, we present performance analysis of algorithmic noise-tolerance (ANT) techniques. First, we analyze the predictor and RPR based ANT schemes. Next, we present a hybrid ANT scheme which is resilient to burst errors usually occurring in a high soft-error rate (P_{er}) region. For a frequency selective FIR filtering, it is shown that simulation results match well with the analytic bounds while providing about 40 dB improvement in the mean square error over a conventional DSP system at a $P_{er} = 10^{-4}$. It is also shown that the proposed hybrid ANT scheme maintains its robustness in noise mitigation even in the high soft-error rate region of upto $P_{er} = 10^{-2}$.

1. INTRODUCTION

We have shown in the past that algorithmic noise-tolerance (ANT) technique [3]-[5] are very effective in combating deep submicron (DSM) noise [1]-[2]. However, past work has focused on simulations to prove the effectiveness of ANT. This paper has two contributions: 1) performance analysis of two existing ANT techniques, the prediction based [3] and reduced-precision redundancy (RPR) [5], and 2) a new ANT technique that is referred to as hybrid ANT and its performance analysis. This paper is organized as follows. After discussing ANT scheme in Section II, we present its performance analysis and propose hybrid ANT scheme in Section III. Simulation results and discussion are given in Section IV.

2. PRELIMINARIES

We first present the ANT based digital signal processing (DSP) system that ensures high reliability in the presence of DSM noise and briefly discuss previous ANT schemes.

2.1. ANT based DSP system

The output of a DSP system is represented by

$$y_{o,n} = d_n + Q_n \tag{1}$$

where d_n is desired output signal and Q_n is the noise due to channel effects, ADC quantization noise, etc.. The output SNR is

$$SNR_{out,org} = 10\log_{10}(\frac{\sigma_d^2}{\sigma_Q^2}) \tag{2}$$

This work is supported by NSF grant CCR 99-79381, ITR 00-85929 and DARPA MSP grant

The output in the presence of soft errors is

$$y_{a,n} = d_n + Q_n + \eta_n \tag{3}$$

where $\eta[n]$ is the noise due to the soft error. In this case, the output SNR is

$$SNR_{out,err} = 10\log_{10}(\frac{\sigma_d^2}{\sigma_Q^2 + \sigma_\eta^2}) \tag{4}$$

where $Q[n]$ and $\eta[n]$ are assumed to be uncorrelated. Equation (4) can be rewritten as $SNR_{out,err} = SNR_{out,org} - \Delta$ where $\Delta = 10\log_{10}(1+\frac{\sigma_\eta^2}{\sigma_Q^2})$. By employing ANT, we reduce the noise power due to soft error σ_η^2 and thereby guaranteeing that Δ is sufficiently small.

The decision rule for an ANT-based DSP system is given by

$$\hat{y}_n = \begin{cases} y_{a,n} & \text{if } |y_{a,n} - y_{ANT,n}| \le T_h \\ y_{ANT,n} & \text{if } |y_{a,n} - y_{ANT,n}| > T_h. \end{cases} \tag{5}$$

where T_h is a precomputed threshold and $y_{ANT,n}$ is the corrected output. In order to guarantee that $y_{a,n} = y_{o,n}$ in the absence of errors, the threshold becomes

$$T_h = \max_{\forall\, y_{o,n}} |y_{o,n} - y_{ANT,n}|. \tag{6}$$

In doing so, no false alarms can occur and therefore only three possible cases exist; (1) no error, (2) undetected error, (3) detected error, with P_{ner}, P_{uer}, and P_{der}, being the corresponding probability of occurrence, respectively. The estimation error power is given by

$$\begin{aligned} \sigma_{y_o-\hat{y}}^2 &= E[\,|y_o - \hat{y}|^2\,] \\ &= P_{der}E[\,|y_o - y_{ANT}|^2\,] \\ &+ P_{uer}E[\,|y_o - y_a|^2 \mid (y_a - y_{ANT} \le T_h)\,] \\ &+ P_{ner}E[\,|y_o - y_a|^2\,] \end{aligned} \tag{7}$$

Note that the third term in (7) is zero. Furthermore, we denote the noise power due to ANT σ_{ANT}^2, and soft error power σ_η^2, as

$$\sigma_{ANT}^2 = E[\,|y_o - y_{ANT}|^2] \tag{8}$$

$$\sigma_\eta^2 = E[\,|y_o - y_a|^2 \mid (y_a - y_{ANT} \le T_h)\,] \tag{9}$$

Substituting (8) and (9) in (7), we get

$$\sigma_{y_o-\hat{y}}^2 = P_{der}\cdot\sigma_{ANT}^2 + P_{uer}\cdot\sigma_\eta^2 \tag{10}$$

0-7803-7761-3/03/$17.00 ©2003 IEEE

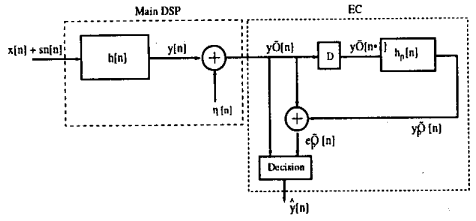

(a)

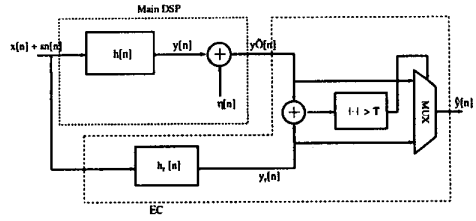

(b)

Figure 1: Algorithmic noise-tolerance schemes: (a) prediction based ANT scheme, and (b) RPR based ANT.

2.2. Prediction based ANT

The block diagram of predictor based ANT is shown in Fig. 1(a), where a forward predictor is added to the original system for error detection and correction [3]. Since the adjacent output y_n, of MDSP is highly correlated for a sufficiently narrowband system, the predictor generates an estimate to be used as an output when an error occurs.

2.3. RPR based ANT

Figure 1(b) shows the block diagram of an RPR based ANT scheme. The RPR is a replica of the original system with small precision operands [5]. Though RPR output $y_{r,n}$ is generally not equal to the original one $y_{o,n}$ due to the LSB quantization noise, it is a good estimate in case of an error event. When an error is detected using (5), $y_{r,n}$ is employed as the final output.

3. PERFORMANCE ANALYSIS OF ANT

In this section, we present an analysis of the predictor, RPR and the hybrid ANT technique which is composed of both techniques. Here, we assume that the error-control block is designed to be error free. Indeed, this assumption is reasonable since the complexity of the error control block is much lesser than that of MDSP and hence the likelihood of soft-error is significantly smaller.

3.1. Predictor based ANT

Let the output vector of an original system is $\boldsymbol{Y} = [y_{n-1}, \ldots, y_{n-N}]^T$ and the predictor coefficient vector is $\boldsymbol{W} = [w_1, \ldots, w_N]^T$. Then, the forward predictor output is

$$y_{p,n} = \sum_{k=0}^{N} w_k y_{n-k-1} = \boldsymbol{W}^T \boldsymbol{Y} \tag{11}$$

where the prediction error $e_{p,n} = y_n - \boldsymbol{W}^T \boldsymbol{Y}$.

By using the derivative of $E[e_{p,n}^2]$, we can show the minimum MSE which corresponds to noise power of forward predictor $\sigma^2_{ANT,pre}$, is given by

$$\sigma^2_{ANT,pre} = \min E[e_{p,n}^2] = E[y_n^2] - \boldsymbol{P}^T \boldsymbol{R}^{-1} \boldsymbol{P} \tag{12}$$

where

$$\begin{aligned} \boldsymbol{P}^T &= E[y_n \boldsymbol{Y}^T] = E[(\, y_n y_{n-1} \cdots y_n y_{n-N}\,)^T] \\ \boldsymbol{R} &= E[\boldsymbol{Y}\boldsymbol{Y}^T] = E[\,(y_{n-1} \cdots y_{n-N})^T (y_{n-1} \cdots y_{n-N})\,] \end{aligned}$$

In addition, by applying the Triangular inequality, we can obtain the upper bound on σ_η^2 as

$$\begin{aligned} \sigma_\eta^2 &= E[\,|y_a - y_o|^2 \mid (y_a - y_{pre} \le T_{h,pre})\,] \\ &= E[\,|y_a - y_{pre} + y_{pre} - y_o|^2 \mid (y_a - y_{pre} \le T_{h,pre})\,] \\ &\le T^2_{h,pre} + \sigma^2_{ANT,pre} \end{aligned} \tag{13}$$

Inserting (12) and (13) into (10), we get the upper bound on the minimum noise power for the prediction based ANT system as

$$\sigma^2_{y_o - \hat{y}} \le P_{der}\, \sigma^2_{ANT,pre} + P_{uer}(T^2_{h,pre} + \sigma^2_{ANT,pre}) \tag{14}$$

Predictor based ANT works well in narrowband systems (typically $\omega_b < 0.3\pi$). However, its prediction performance reduces when the filter bandwidth increases. In addition, when a burst error occurs in the system, as would be the case in high P_{er} region, the predictor cannot provide reliable detection thereby degrading the system performance severely.

3.2. RPR based ANT

Assume that the operands precision in a reference original system is $B_1 + 1$ bits and that of a RPR system is $B_2 + 1$ bits, where $B_1 > B_2$. In addition, we denote the quantization step size of an original DSP and that of RPR as $\Delta_o = \frac{1}{2^{B_1}}$ and $\Delta_r = \frac{1}{2^{B_2}}$. The quantization noise N_x and N_h between the original value and that of RPR x_r and h_r is defined as $N_x = x - x_r$ and $N_h = h - h_r$, where x and h are the input and filter coefficients, respectively. With this assumption, one can show that the noise power of the RPR ANT scheme $\sigma^2_{ANT,rpr}$, is given by

$$\sigma^2_{ANT,rpr} = \sum_i [N^2_{h_i} \sigma_x^2 + \frac{h^2_{r,i}}{6}(2\Delta_r^2 - 3\Delta_r \Delta_o + \Delta_o^2)] \tag{15}$$

where σ_x^2 is the input signal power. By applying an analysis similar to the one in (13), we get the noise power σ_η^2 as

$$\sigma_\eta^2 \le T^2_{h,rpr} + \sigma^2_{ANT,rpr} \tag{16}$$

Employing (15), (16), and (10) we can obtain the upper bound on the noise power for the RPR based ANT as

$$\begin{aligned} \sigma^2_{y_o - \hat{y}} &= P_{der} \cdot \sigma^2_{ANT,rpr} + P_{uer} \cdot \sigma_\eta^2 \\ &\le P_{der} \cdot \sigma^2_{ANT,rpr} + P_{uer} \cdot (T^2_{h,rpr} + \sigma^2_{ANT,rpr}) \end{aligned} \tag{17}$$

Note that the noise power term in (17) depends only on precision and quantization noise but not on bandwidth. While the RPR based ANT provides good performance for a wide range of bandwidths, it consumes more power than the predictor based ANT system.

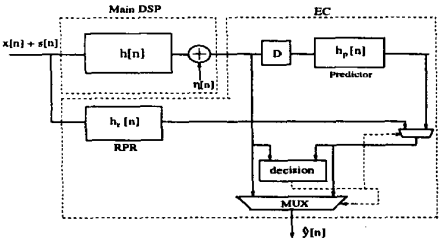

(a)

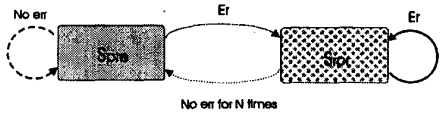

(b)

Figure 2: The hybrid ANT technique: (a) block diagram, and (b) the state machine.

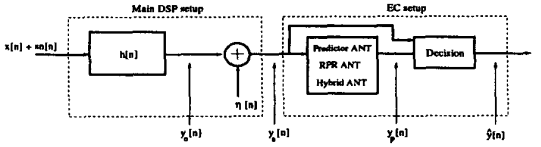

Figure 3: Simulation setup.

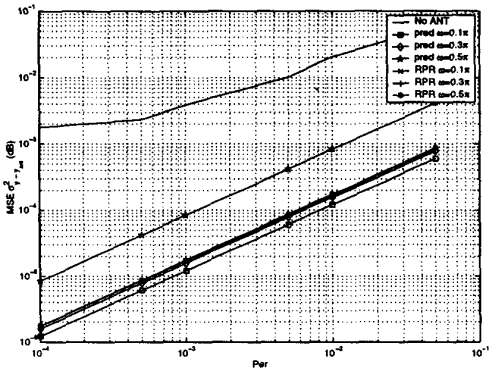

Figure 4: Analytic results of prediction and RPR ANT scheme for bandwidth variation.

3.3. Hybrid ANT

The predictor based ANT, which produces good performance in low soft-error rate P_{er}, has a problem as P_{er} increases. Once error is made, an erroneous output is fed back into the predictor, leading to an incorrect decision until the erroneous output is purged. On the other hand, the RPR based ANT has relatively high power consumption than the predictor based scheme.

Figure 2(a) shows the block diagram of the proposed hybrid ANT scheme that overcomes this problem. The key idea in the hybrid ANT is to use a predictor when there are no errors (i.e., for error detection) and RPR when an error occurs (i.e., error correction). As illustrated in Fig. 2(b), the error control is transferred to an RPR state (S_{rpr}) from a predictor state (S_{pre}) after error detection. If RPR does not detect an error for N consecutive cycles, i.e., the error propagation is terminated, then the error control is passed back to the predictor.

Assuming that the error event is independent, the probability of being in the RPR and predictor states are, respectively,

$$\begin{aligned} P_{rpr} &= P_{er} + (1-P_{er})P_{er} + \cdots (1-P_{er})^{N_p-1}P_{er} \\ P_{pre} &= (1-P_{er})^{N_p} \end{aligned} \tag{18}$$

where N_p is the number of taps in the predictor. Clearly, $P_{rpr} + P_{pre} = 1$. Then, the noise power of the hybrid ANT system is

$$\sigma^2_{ANT,hybrid} = P_{rpr}\,\sigma^2_{ANT,rpr} + P_{pre}\,\sigma^2_{ANT,pre} \tag{19}$$

Using (18), (19), and (14), we can obtain the upper bound on the noise power of the hybrid ANT as

$$\begin{aligned} \sigma^2_{y_o-\hat{y}} \;\leq\; & P_{der}P_{pre}\cdot\sigma^2_{ANT,pred} + P_{der}P_{rpr}\cdot\sigma^2_{ANT,rpr} \\ + \;& P_{uer}P_{pre}\cdot(T^2_{h,pre}+\sigma^2_{ANT,pre}) \\ + \;& P_{uer}P_{rpr}\cdot(T^2_{h,rpr}+\sigma^2_{ANT,rpr}) \end{aligned} \tag{20}$$

Since RPR is used only when error is detected, we can turn this block off in the predictor state S_{pre} and thereby save power while maintaining robustness when P_{er} is high.

4. SIMULATIONS AND DISCUSSION

The setup used to measure the performance of the proposed scheme is shown in Fig. 3, where a frequency selective filter is used to generate a bandlimited signal $y_o[n]$ from a wideband input with noise $x[n] + s[n]$. The SNR without ANT is given by

$$SNR_{in} = 10\log_{10}\frac{\sigma^2_{y_o}}{\sigma^2_{y_a-y_o}} \tag{21}$$

whereas, the SNR at the ANT output is given by

$$SNR_{out} = 10\log_{10}\frac{\sigma^2_{y_o}}{\sigma^2_{y_o-\hat{y}}} \tag{22}$$

where $\sigma^2_{y_o}$, is the signal power of original filter output. In this simulation, we employ a 31-tap filter with a 12×12 multipliers and a 26-bit accumulator. For a DSM noise model, we employ random flipping of an output bit in the digital filter with a specified soft-error probability P_{er}. Figure 4 shows the analysis results of predictor and RPR based ANT, where the main filter is a low-pass filter having a bandwidth from $\omega_b = 0.1\pi$ to 0.5π. For the RPR MAC, we used the half precision of the original filter (i.e., 6×6 multiplier) and a three tap of predictor is employed in the prediction based ANT. While the performance of RPR is quite similar

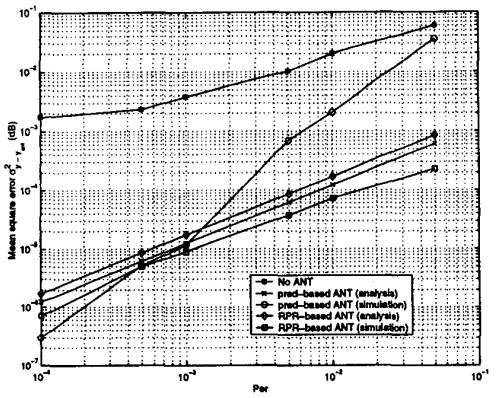

Figure 5: Performance analysis and simulation results of prediction and RPR ANT scheme.

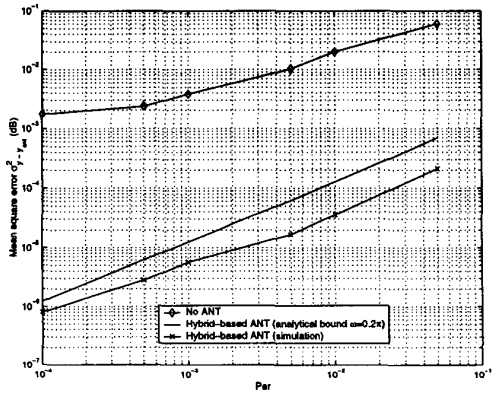

Figure 6: Performance analysis and simulation results of hybrid ANT scheme.

over the entire frequency range, the performance of the predictor deteriorates as the bandwidth increases.

Figure 5 shows the analysis and simulation results of the predictor and RPR based ANT, where the bandwidth of main filter is now set to $\omega_b = 0.2\pi$. While the conventional system has high mean square error regardless of P_{er}, predictor ANT has MSE less than 10^{-6} at $P_{er} = 10^{-4}$ resulting in 40 dB gain over conventional MDSP. As discussed in Section II.A, the performance of predictor degrades severely as P_{er} increases due to the error propagation. On the contrary, the performance of RPR is close to the analytic results even when P_{er} is high.

Next, we considered the hybrid ANT scheme under the same simulation setup. As shown in Fig. 6, the performance of hybrid ANT is similar to the prediction scheme in low P_{er} region. However, unlike to prediction scheme, we observe that hybrid scheme maintains its performance even when P_{er} becomes high.

Finally, in order to observe the comprehensive picture including additional power consumption, we show the contour plot for the power overhead as well as P_{er}, which is given by

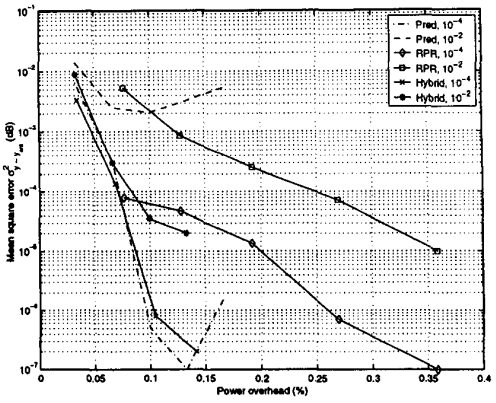

Figure 7: Contour plot for P_{er} and power overhead variation.

$$P_{overhead}(\%) = \frac{P_{ANT} - P_{MDSP}}{P_{MDSP}} \times 100\%. \qquad (23)$$

where P_{MDSP} and P_{ANT} are the power of original DSP and ANT based DSP, respectively. As shown in Fig. 7, the power overhead of hybrid ANT is about $15 \sim 20$ % lesser than that of RPR in a similar MSE region. Thus, the hybrid ANT scheme is not only robust to soft-errors when P_{err} is high, it is also energy-efficient.

5. REFERENCES

[1] T. Karnik and S. Vangal, "Selective node engineering for chip-level soft error rate improvement," *Proc. of Symp. on VLSI circuits*, vol. 4, pp. 132-135, 2002.

[2] N. Shanbhag, K. Soumyanath, and S. Martin, "Reliable low-power design in the presence of deep submicron noise," *Proc. of Intl. Symp. on Low-Power Electronics and Design*, pp 295-302, 2000.

[3] R. Hedge and N. Shanbhag, "Soft digital signal processing," *IEEE Trans. VLSI*, vol. 9, pp. 813-823, Dec. 2001.

[4] L. Wang and N. Shanbhag, "Low-power signal processing via error-cancellation," *Proc. of IEEE workshop on Signal Processing Systems*, Lafayette Oct. 2000.

[5] B. Shim, and N. R. Shanbhag, "Low-power digital filtering via reduced-precision redundancy," *Proc. of Asilomar conf.*, Vol. 1, pp. 148-152, Nov. 2001.